Supplementary Materials

Quantitative Gradient Echo MRI Identifies Dark Matter as a New Imaging Biomarker of Neurodegeneration that Precedes Tissue Atrophy in Early Alzheimer Disease

Satya V.V.N. **Kothapalli**[1], Tammie. L. **Benzinger**[1, 2], Andrew. J. **Aschenbrenner**[2, 3], Richard. J. **Perrin**[2,3,4,5], Charles. F. **Hildebolt**[1], Manu. S. **Goyal**[1, 3], Anne. M. **Fagan**[2, 3,5], Marcus. E. **Raichle**[1,3,5], John. C. **Morris**[2, 3], and Dmitriy. A. **Yablonskiy**[1,2,5,*]

[1]Department of Radiology, Washington University in St. Louis, St. Louis, MO 63110, USA.

[2]Knight Alzheimer Disease Research Center, Washington University in St. Louis, St. Louis, MO 63110, USA.

[3]Department of Neurology, Washington University in St. Louis, St. Louis, MO 63110, USA.

[4]Department of Pathology and Immunology, Washington University in St. Louis, St. Louis, MO 63110, USA.

[5]The Hope Center for Neurological Disorders, Washington University in St. Louis, St. Louis, MO, USA

*Correspondence to:

Dmitriy A. Yablonskiy, PhD

Mallinckrodt Institute of Radiology, Washington University, 4525 Scott Ave. Room 3216

St. Louis MO, 63110

Email: yablonskiyd@wustl.edu

Tel.: +1(314)362-1815; Fax: +1(314)362-0526

Running title : **Brain Dark Matter - Biomarker of Alzheimer Disease**

Supplementary Materials

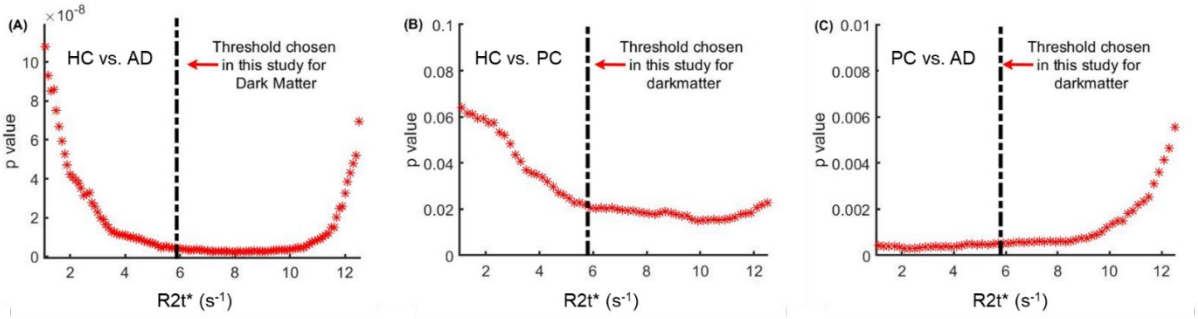

Supplementary Figure 1. The choice of R2t* threshold for justifying the separation of Dark Matter volume from Viable tissue volume. Plots show dependencies of p value defining significance of group differences between (A) HC and mild AD groups, (B) HC and PC groups, and (C) mild AD and PC groups (using Dark Matter volume as a variable) with varying R2t* threshold (from 1.1 s^{-1} to 12.5 s^{-1} with a step size of 0.1 s^{-1}) separating Dark Matter and Viable Tissue. p values obtained from HC and mild AD group comparison, were decreasing with increasing R2t* from 1.1 s^{-1} to 4 s^{-1}, remained relatively stable between R2t* of 4 s^{-1} and 10.5 s^{-1} and then started to increase with increasing R2t*. The p values between HC and PC groups were decreasing with increasing R2t* threshold and saturated around 6 s^{-1} till 12.5 s^{-1} and the p values between mild AD and PC groups were small and relatively stable for R2t* values less than ~9 s^{-1} and then sharply increased above 9 s^{-1}. This result illustrates that the R2t*=5.8 s^{-1} threshold for Dark Matter separation is a reasonable criterion for assessment in AD-related participants.

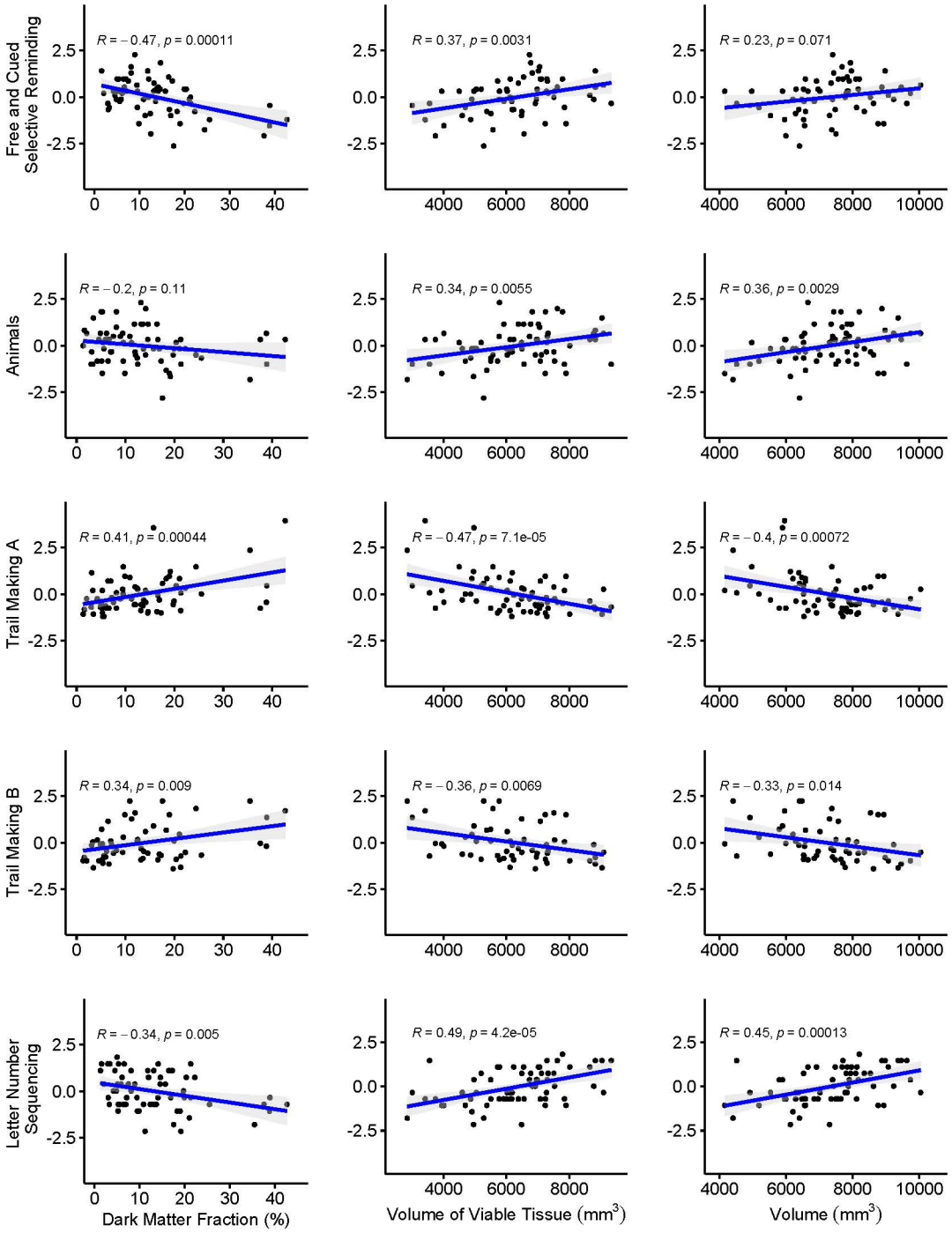

Supplementary Figure 2. Correlation of individual neurocognitive tests with fraction of Dark Matter, volume of Viable Tissue, and Total Volume of the hippocampus. Each point represents an individual participant.

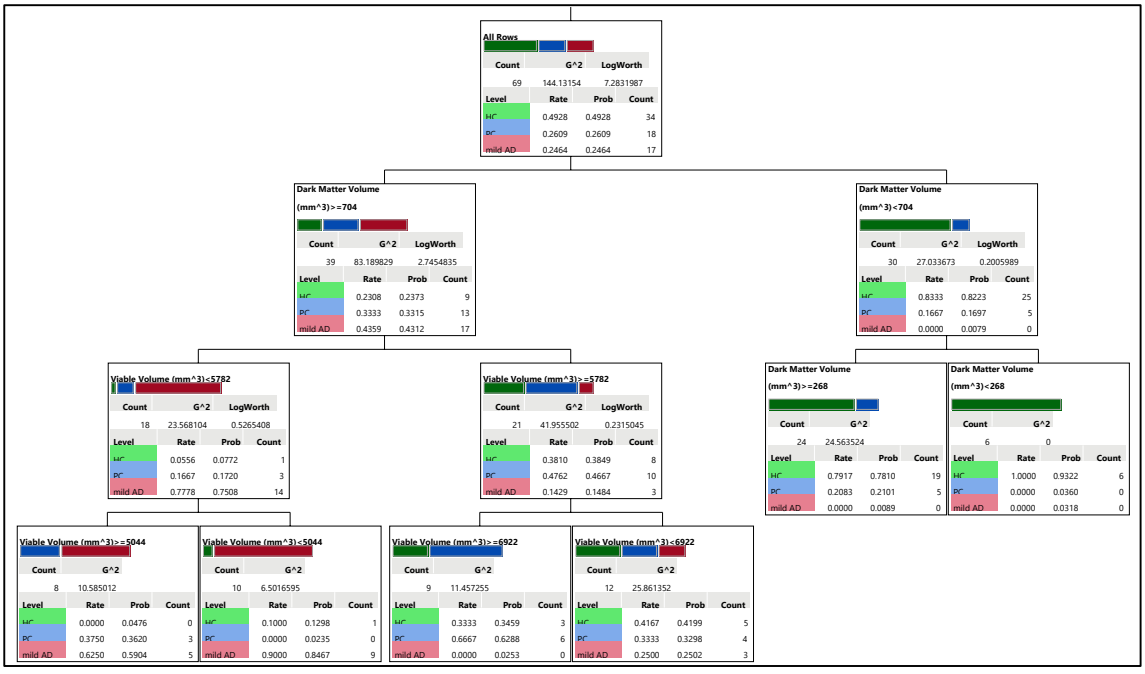

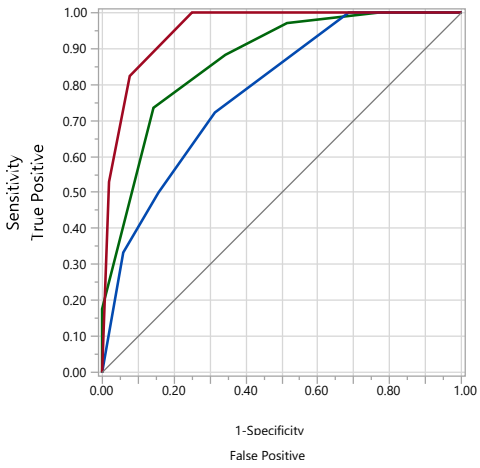

STATUS	Area
HC	0.8676
PC	0.7810
mild AD	0.9519

Confusion Matrix

Actual	Predicted Count		
STATUS	**HC**	**PC**	**AD**
HC	30	3	1
PC	9	6	3
mild AD	3	0	14

Column Contributions

Term	Number of Splits	G^2		Portion
Dark Matter	2	36.3781924		0.5583
Viable Volume	3	28.7845509		0.4417

Supplementary Figure 3. Results of a classification-tree that was produced using global hippocampal Dark Matter volume and Viable Tissue volume variables as predictors. The top panel presents the classification tree diagram with threshold's, middle panel presents receiver operating characteristic (ROC) curves and areas under the curves (AUCs), a confusion matrix, and bottom panel presents the contribution of variables in the classification of HC, PC, and AD groups. The confusion matrix presents the numbers of correct and incorrect classifications.

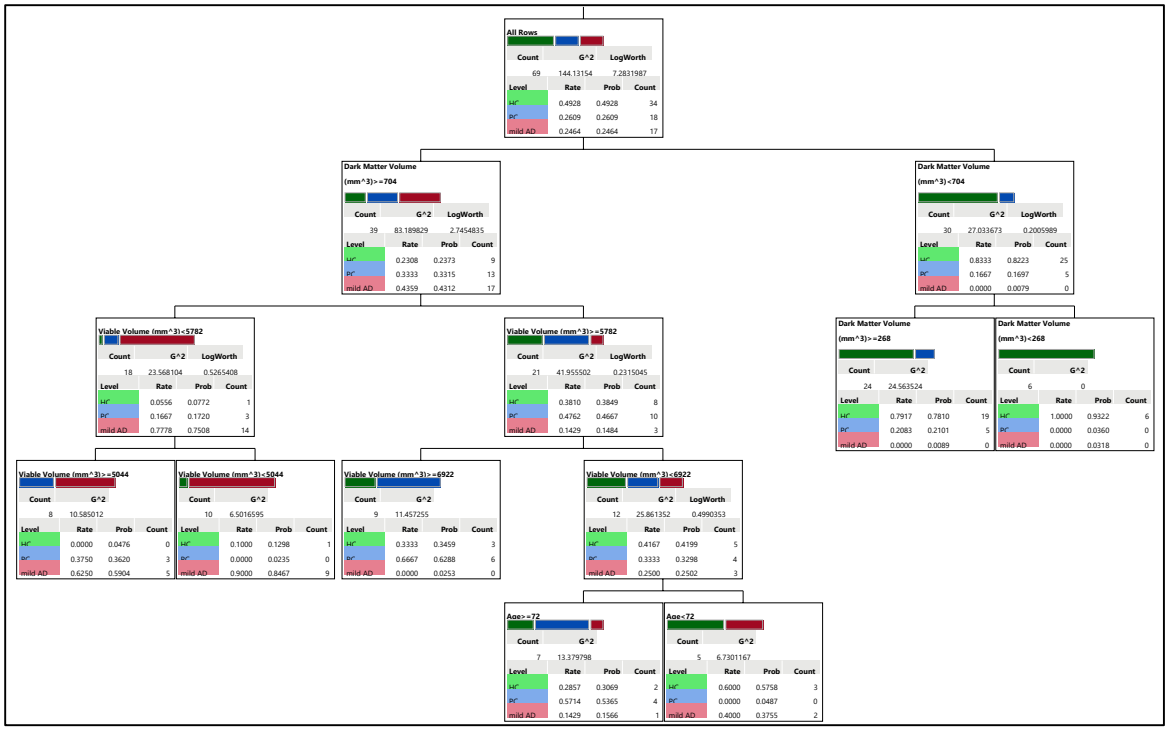

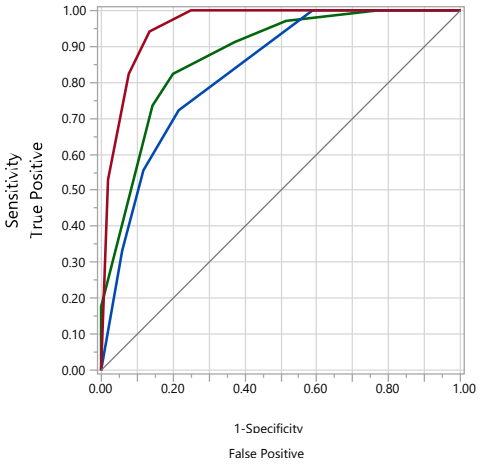

STATUS	Area
HC	0.8748
PC	0.8312
mild AD	0.9570

Confusion Matrix

Actual STATUS	Predicted Count HC	PC	AD
HC	28	5	1
PC	5	10	3
mild AD	2	1	14

Column Contributions

Term	Number of Splits	G^2	Portion
Viable Volume	2	36.3781924	0.5130
Dark Matter	2	10.6888841	0.2190
Age	1	5.7514367	0.0811

Supplementary Figure 4. Results of a classification-tree that was produced using global hippocampal Dark Matter volume, Viable Tissue volume, and participant's age variables as predictors. The top panel presents the classification tree diagram with threshold's, middle panel presents receiver operating characteristic (ROC) curves and areas under the curves (AUCs), a confusion matrix, and bottom panel presents the contribution of variables in the classification of HC, PC, and AD groups. The confusion matrix presents the numbers of correct and incorrect classifications.

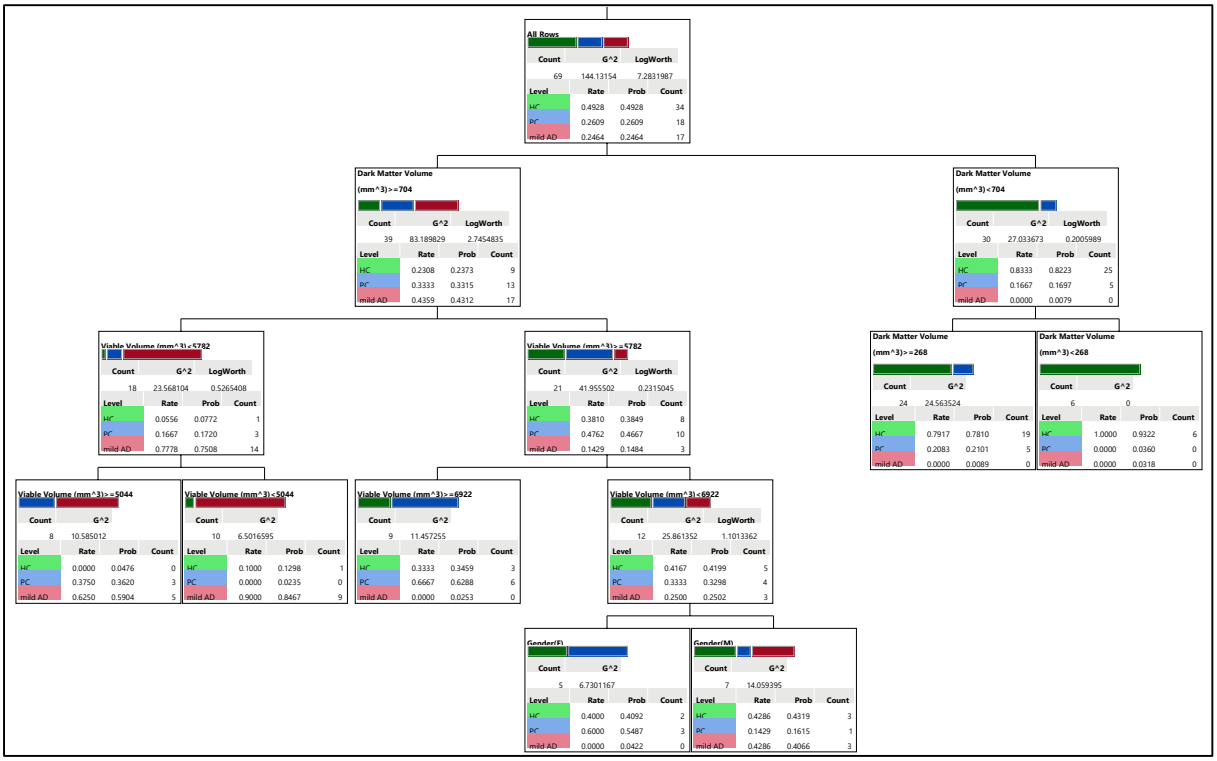

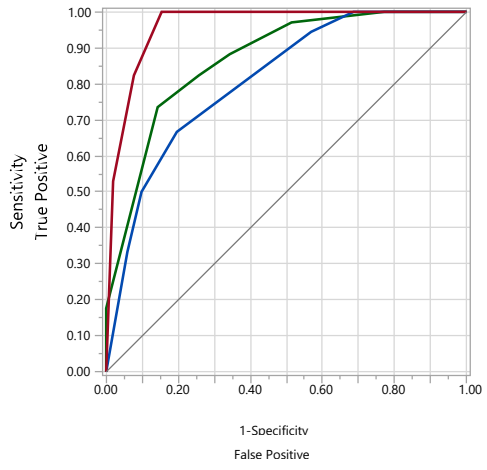

STATUS	Area
HC	0.8681
PC	0.8115
AD	0.9604

Confusion Matrix

Actual STATUS	Predicted Count HC	PC	AD
HC	28	5	1
PC	6	9	3
AD	3	0	14

Column Contributions

Term	Number of Splits	G^2	Portion
Viable Volume	3	28.7845509	0.4098
Dark Matter	2	36.3781924	0.5180
Gender	1	5.07184056	0.0722

Supplementary Figure 5. Results of a classification-tree that was produced using global hippocampal Dark Matter volume, Viable Tissue volume, and Gender variables as predictors. The top panel presents the classification tree diagram with threshold's, middle panel presents receiver operating characteristic (ROC) curves and areas under the curves (AUCs), a confusion matrix, and bottom panel presents the contribution of variables in the classification of HC, PC, and AD groups. The confusion matrix presents the numbers of correct and incorrect classifications.

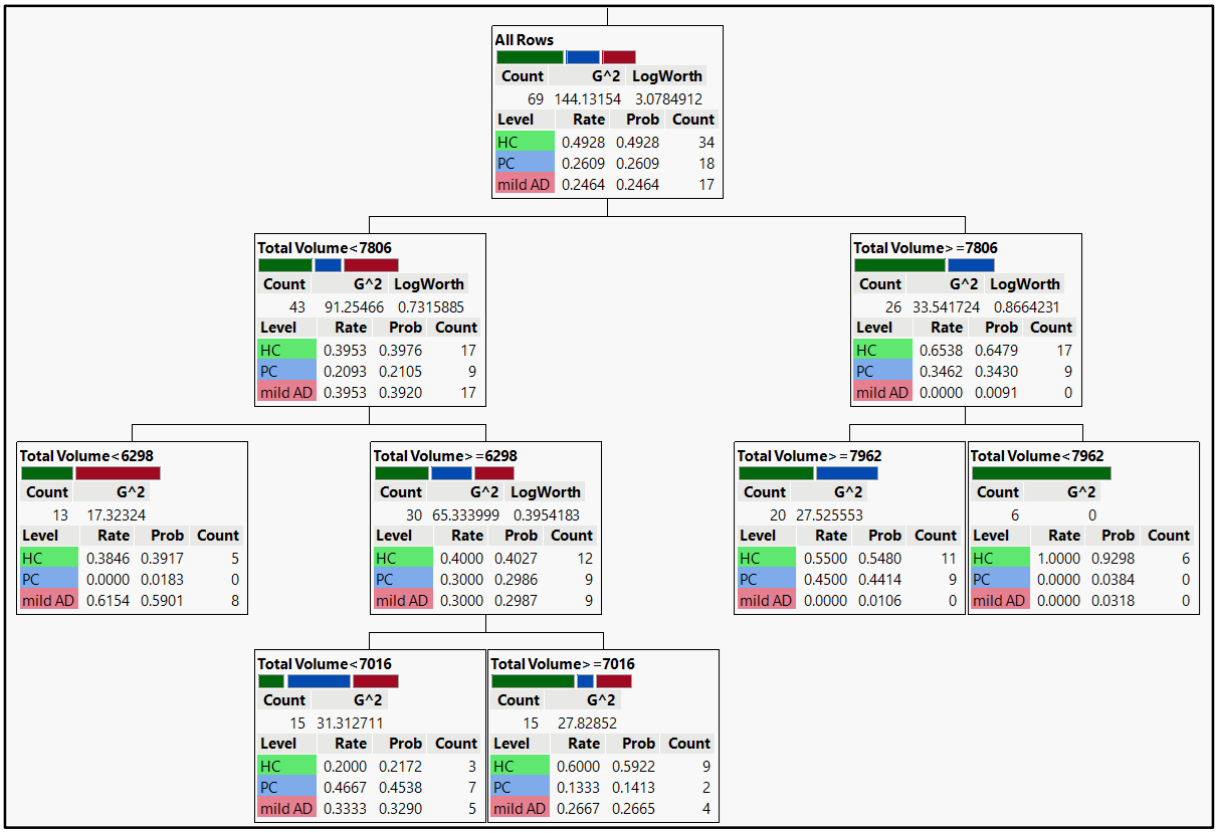

Supplementary Figure 6. Results of a classification-tree that was produced using hippocampal Total Volume variable as a predictor. The top panel presents the classification tree diagram with threshold's, lower panel presents receiver operating characteristic (ROC) curves, areas under the curves (AUCs), and a confusion matrix. The confusion matrix presents the numbers of correct and incorrect classifications.

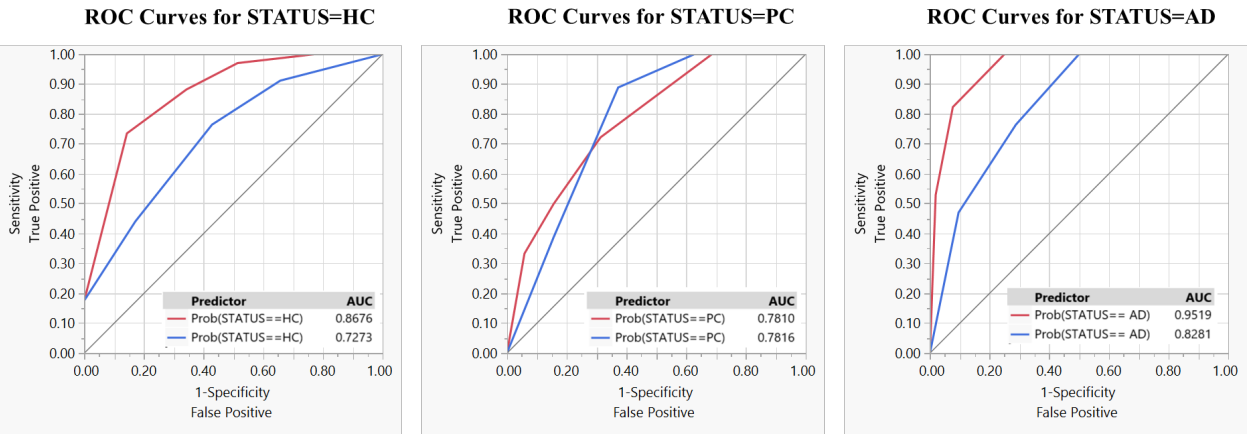

Supplementary Figure 7. ROC-curve comparisons for classification results based on qGRE metrics versus commonly used tissue atrophy. The comparison of ROC curves created with Dark Matter & Viable Volume versus Total Volume. The red lines represent Volumes of Dark Matter and Viable Tissue used as predictors, and the blue lines represent Total Volume used as a predictor. Insets show corresponding AUC values.

Significant differences in the AUC values for the ROC curves were found for HC ($p = 0.0304$) and mild AD ($p = 0.0016$). For HC Dark Matter and Viable Tissue volumes AUC was 0.8676 (0.7662 – 0.9291, 95% confidence interval (CI)) and for Total Volume the AUC value was 0.7273 (0.5989 – 0.8265, 95% CI) with $p = 0.0304$. The corresponding results for PC were 0.7810 (0.6496 – 0.8729, 95% CI) and 0.7816 (0.6636 – 0.8665, 95% CI), $p = 0.9940$, and for mild AD, 0. 9519 (0.8838 – 0.8910, 95% CI) and 0.8281 (0.7129 – 0.9033, 95% CI), $p = 0.0016$.

Supplementary Table 1. Statistical analysis of the potential influences of MRI scanners on the data obtained in this study. In this study, the data acquired on four different Siemens 3T MRI scanners (PET-MR, Prisma, Trio, and VIDA). The Fisher-Freeman-Hatton test is an extension of the Fisher's exact test to an unordered r x c table for the three groups of participants (HC, PC, and mild AD) and four different MRI scanners were used (PET-MR, Prisma, Trio, and VIDA). The Count, Total%, Col% (column percent), and Row% correspond to the data within each cell that has row and column headings (such as the cell under PET-MR and HC). The Fisher-Freeman-Hatton test demonstrated that the three groups of participants (HC, PC, and mild AD) were independent ($P = 0.2096$) of the four different MRI scanners (PET-MR, Prisma, Trio, and VIDA).

Count Total % Col % Row %	PET-MR	Prisma	Trio	VIDA	Total
HC	5 7.14 31.25 14.71	16 22.86 64.00 47.06	4 5.71 40.00 11.76	9 12.86 47.37 26.47	34 48.57
mild AD	7 10.00 43.75 41.18	5 7.14 20.00 29.41	1 1.43 10.00 5.88	4 5.71 21.05 23.53	17 24.29
PC	4 5.71 25.00 21.05	4 5.71 16.00 21.05	5 7.14 50.00 26.32	6 8.57 31.58 31.58	19 27.14
Total	16 22.86	25 35.71	10 14.29	19 27.14	70

Supplementary Table 2. Mean values and standard deviations (STD) of R2t* distributions for three groups in Dark Matter (R2t*<5.8 s^{-1}), and Viable Tissue (R2t*>5.8 s^{-1}).

Groups	Dark Matter R2t* (s^{-1})		Viable tissue R2t* (s^{-1})	
	Mean	**STD**	**Mean**	**STD**
AD	2.2	1.6	14.3	4.8
PC	2.3	1.6	14.9	4.8
HC	2.7	1.7	15.2	4.3

Supplementary Table 3. Summary of mean neuronal count and Dark Matter measurements in five hippocampal subfields. Neuron counts were performed by a highly experienced board-certified neuropathologist, blinded to any neuroimaging data or formal neuropathologic diagnosis at the time of cell counting. Three 40x objective fields (each 0.55 mm diameter) selected for counting were evenly spaced but otherwise randomly chosen within each area of interest based on boundaries borrowed from FreeSurfer. Neurons were identified by morphology on H&E stained slides. Plot on the wright illustrates an association between actual neuronal count and fraction of Dark Matter in the corresponding regions of hippocampus.

Hippocampal subfields	Neurons per objective field	Dark Matter fraction
CA4	21	10%
CA2/CA3	59	3%
CA1	3	23%
Subiculum	1	18%
Parasubiculum	8	25%